Available online at www.sciencedirect.com
ScienceDirect
International Journal of Heat and Mass Transfer 50 (2007) 4796–4804
International Journal of HEAT and MASS TRANSFER
www.elsevier.com/locate/ijhmt

Convective gas cooling heat transfer and pressure drop characteristics of supercritical CO_2/oil mixture in a minichannel tube

Rin Yun [a], Yunho Hwang [b,*], Reinhard Radermacher [b]

[a] Department of Mechanical Engineering, Hanbat National University, San 16-1, Duckmyung-dong, Yuseong-gu, Daejeon 305-719, Republic of Korea
[b] Center for Environmental Energy Engineering, Department of Mechanical Engineering, University of Maryland, 3163 Glenn Martin Hall Building, College Park, MD 20742, USA

Received 25 October 2006; received in revised form 25 February 2007
Available online 9 May 2007

Abstract

The effects of PAG oil concentration on the convective gas cooling heat transfer and the pressure drop characteristics of supercritical CO_2/oil mixture in minichannel tube were investigated. The test results showed that the average gas cooling heat transfer coefficient was decreased by 20.4% and the average pressure drop was increased by 4.8 times when the oil concentration was increased from 0 to 4 wt.%. The effects of the oil concentration on the convective gas cooling heat transfers and the pressure drops of the supercritical CO_2/oil mixture in minichannel tubes were experimentally confirmed to be significant.

Keywords: CO_2; Gas cooling; Oil; Oil concentration; Heat transfer coefficient; Pressure drop

1. Introduction

CO_2 has been reinvestigated as a working fluid for various refrigeration and air conditioning systems such as mobile and residential air-conditioners and heat pump water heaters, due to the escalating environmental concerns. There have been many studies to improve the efficiency of the transcritical CO_2 cycle to an equivalent or to even a better level than that of the systems using conventional refrigerants. As a result, the performance of the transcritical CO_2 cycle has been significantly improved by adapting various advanced components and cycle options such as a minichannel heat exchanger, an expander, an ejector, an internal heat exchanger, and multi-stage cycles. Among these, the CO_2 system operating at relatively high pressures than the conventional refrigerant systems can favorably utilizes the minichannel heat exchangers as its gas cooler and evaporator due to its high density. Moreover, the CO_2 cycle has smaller vapor and liquid density ratios than those of the conventional refrigerants, so that it experiences less mal-distribution between the liquid and vapor phases in the minichannel heat exchanger. During the operation of the vapor compression cycle, the oil circulates through all components of the system though the oil is only needed in the compressor. The lubricating oil in the heat exchangers deteriorates the heat transfer performance and increases the pressure drop. Its impact is especially greater in the minichannel heat exchangers than in the conventional fin-and-tube heat exchangers since the oil can block some minichannel ports. Therefore, understanding the effects of the oil on the heat transfer coefficient and the pressure drop is essential in developing minichannel heat exchangers appropriate to the transcritical CO_2 cycle. These issues were investigated by many researchers as summarized below.

Pitla et al. [1] reviewed the studies of the heat transfer characteristics of CO_2 in tube gas cooling at the supercritical state. In the supercritical region, the large variations in the thermophysical properties of the fluid strongly affect the heat transfer characteristics. Olson and Allen [2], Yoon et al. [3], Son and Park [4], Dang and Hihara [5], and Liao

* Corresponding author. Tel.: +1 301 405 5247; fax: +1 301 405 2025.
E-mail address: yhhwang@eng.umd.edu (Y. Hwang).

0017-9310/$ - see front matter © 2007 Elsevier Ltd. All rights reserved.
doi:10.1016/j.ijheatmasstransfer.2007.03.018

Nomenclature

A	area, m^2
AN	alkyl naphthalene
c_p	specific heat, J/kg K
d_h	hydraulic diameter, m
G	mass flux, kg/m^2 s
h	heat transfer coefficient, W/m^2 K
ID	inner diameter, m
k	thermal conductivity, W/m K
K_L	geometrical minor losses
L	length, m
$\dot{m}$	mass flow rate, kg/s
P	pressure, kPa
PAG	polyalkylenglycol
POE	polyolester
Pr	Prandtl number
$\dot{q}$	heat transfer rate, W
Re	Reynolds number
T	temperature, K

Greek symbols

Δ	difference
ρ	density, kg/m^3
μ	dynamic viscosity, N s/m^2
ω	bulk oil mass concentration in the total mixture, wt.%

Subscripts

avg	average
in	inlet
lmtd	log mean temperature difference
mix	mixture

and Zhao [6] experimentally investigated the gas cooling heat transfer coefficients and pressure drops of supercritical CO_2 in the horizontal tubes with the test conditions as shown in Table 1. The authors compared the experimental results with the existing correlations and found that when the diameter of the test tubes was larger than 2.0 mm, the deviation between the experimental data and the predicted results were less than 20%. However, the existing correlations failed to predict the experimental results when the diameter of the test tubes is less than 2.0 mm. Liao and Zhao [7], and Dang and Hihara [8] also numerically investigated the gas cooling heat transfer characteristics of CO_2 at supercritical condition. Liao and Zhao [7] found that the buoyancy effect was significant on the heat transfer in vertical mini tubes. Dang and Hihara [8] tested four different turbulence models by comparing each numerical result with the experimental data. The $k-\varepsilon$ model by Jones and Launder showed the best agreement with the experimental data. Pettersen et al. [9] studied gas cooling heat transfer and pressure drop characteristics of pure CO_2 in minichannels with a diameter of 0.79 mm. They reported that the Gnielinski heat transfer model and the Colebrook-and-White pressure drop model predicted the test results with 4% and 2% of the mean deviation, respectively. Kuang et al. [10] also compared their test results of gas cooling heat transfer coefficients of pure CO_2 in minichannels with the Gnielinski model. The model predicted their experimental results within 10% of mean deviation in a low mass flux range. However, in a high mass flux region, the mean deviations between the test results and the predicted data were as much as 60%. Dang et al. [11] visualized supercritical CO_2 with a small amount of PAG oil by using a sight glass in a tube with an inner diameter of 2 mm. At a low CO_2 temperature of 30 °C and an oil concentration of 1 wt.%, a large number of oil droplets were observed in the flow with CO_2. However, both size and quantity of the oil droplets, which were entrained with CO_2, decreased, and the flow of the oil film became clearly visible with an increase of the CO_2 temperature to 50 °C. Dang et al. [12] also investigated the effects of PAG oil on the gas cooling heat transfer characteristics of supercritical CO_2. The test conditions used are as shown in Table 1. The effects of the oil concentration on the gas cooling heat transfer coefficients and the pressure drops were significant for small sized tubes of 1 or 2 mm. The maximum reduction in the heat transfer coefficients of 75% occurred in the vicinity of the pseudocritical temperature, and the pressure drop increased monotonously with an increase in the oil concentration. Gao and Honda [13] experimentally studied the heat transfer characteristics of CO_2 inside the horizontal tubes, which were used as a gas cooler of a CO_2 heat pump system. When the concentration of lubrication oil was 1 wt.%, the average heat transfer coefficients were about 20% lower than those without oil. Mori et al. [14] studied the gas cooling heat transfer characteristics of supercritical CO_2 with oil. Although the exact oil concentration was not controlled in their study, the heat transfer coefficients of the mixture were lower than those of pure CO_2, particularly near the pseudocritical temperature. Zingerli and Groll [15] measured the heat transfer coefficients and pressure drops of CO_2/oil mixture in a 2.75 mm stainless steel tube. The experiments showed a large decrease in the maximum heat transfer coefficients around the pseudocritical temperature. The tests showed that a 5 wt.% oil concentration reduced the heat transfer coefficients by 25% on average. Kuang et al. [16] investigated the effects of the different types of oil on the gas cooling heat transfer coefficients of CO_2 in minichannel whose hydraulic diameter is 0.79 mm. The oils used in their study were PAG, POE, and AN/PAG. They found that the heat transfer coefficients were reduced up to 57% and the pressure drops increased 44% for 5 wt.% oil concentration.

Table 1
Summary of CO_2 gas cooling heat transfer studies

Authors	Fluids	Tube geometry	Experimental conditions
Pitla et al. [1]	CO_2	Smooth tube, ID: 4.7 mm	T: 20–126 °C P: 8.1–13.4 MPa G: 1100–2200 kg/m^2 s
Olson and Allen [2]	CO_2	Smooth tube, ID: 10.9 mm	T: 20–126 °C P: 7.8–13.1 MPa G: 200–900 kg/m^2 s
Yoon et al. [3]	CO_2	Smooth tube, ID: 7.75 mm	T_{avg}: 50–80 °C P: 7.5–8.8 MPa G: 225, 337, 450 kg/m^2 s
Son and Park [4]	CO_2	Smooth tube, port ID 7.75 mm	T: 25–90 °C P: 7.5–10 MPa G: 200–400 kg/m^2 s
Dang and Hihara [5]	CO_2	Smooth tube, ID: 1–6 mm	T_{in}: 30–70 °C P: 8–10 MPa G: 200–1200 kg/m^2 s
Liao and Zhao [6]	CO_2	Smooth tube, ID: 0.5, 0.7, 1.1, 1.4, 1.55, 2.16 mm	T: 20–110 °C P: 7.4–12.0 MPa G: 136–4244 kg/m^2 s
Pettersen et al. [9]	CO_2	Microchannel, port ID 0.79 mm	T_{avg}: 20–60 °C P: 8.1–10.1 MPa G: 600–1200 kg/m^2 s
Dang et al. [12]	CO_2/PAG	Smooth tube, ID: 1–6 mm	T_{in}: 100–125 °C P: 8–10 MPa G: 200–1200 kg/m^2 s Oil concentration: 0–5 wt.%
Gao and Honda [13]	CO_2/oil	Smooth tube, ID: 5 mm	T: 30–100 °C P: 7.6–9.6 MPa G: 330–680 kg/m^2 s Oil concentration: 0, 1 wt.%
Mori et al. [14]	CO_2/PAG	Smooth tube, ID: 4, 6, 8 mm	T: 20–70 °C P: 9.5 MPa G: 100–500 kg/m^2 s
Zingerli and Groll [15]	CO_2/POE	Smooth tube, ID: 2.75 mm	T_{in}: 100–125 °C P: 8–12 MPa G: 1700–5100 kg/m^2 s Oil concentration: 0, 2 and 5 wt.%
Kuang et al. [16]	CO_2/oils (PAG/AN, PAG, POE)	Microchannel, port ID 0.79 mm	T: 30–50 °C P: 9 MPa G: 890 kg/m^2 s Oil concentration: 0–5 wt.%

However, their tests were conducted under fixed CO_2 pressure and mass flux conditions of 9 MPa and 844 kg/m^{2}s, respectively. The average temperature of CO_2 across a test section was also limited from 30 to 50 °C.

The effects of the test conditions on the gas cooling heat transfer coefficients and the pressure drops of CO_2/oil were not clear in the summarized studies above and their experiments did not control the oil concentration or were limited in the test conditions. The objective of this study is to investigate the effects of PAG oil on the gas cooling heat transfer and the pressure drop of CO_2 in a wider operation conditions, which are determined with the actual system in mind. The effects of mass flux, test section inlet pressure and temperature of CO_2 at various oil concentrations were also investigated too. Additionally the degradation ratio of the heat transfer coefficients due to the oil was compared to the predictions of using the exiting models. Lastly, the effects of the oil on the pressure drops were analyzed by using the modified Darcy–Weisbach model.

2. Experimental set-up

Fig. 1 shows the schematic diagram of the test set-up. Basically, it is composed of two loops: the vapor compression loop and the test section loop. The components of the vapor compression loop are a CO_2 compressor, a gas cooler, expansion valves, and an evaporator. This loop was utilized to attain the target CO_2 mass flux through the test section, and the target temperature and pressure of CO_2 entering the test section. The test section loop consists of the test section, a cooling water loop, and a syringe pump. The CO_2 flow divided from the gas cooler flows into the test section loop. The cooling water circulated through the test section by a pump and removed the heat from the CO_2 undergoing gas cooling process. The temperature of the supply cooling water was set by the constant temperature water bath as shown in Fig. 1. The mass flow rate of CO_2 at the test section was controlled by adjusting the opening of the needle valve. The syringe pump was used to inject

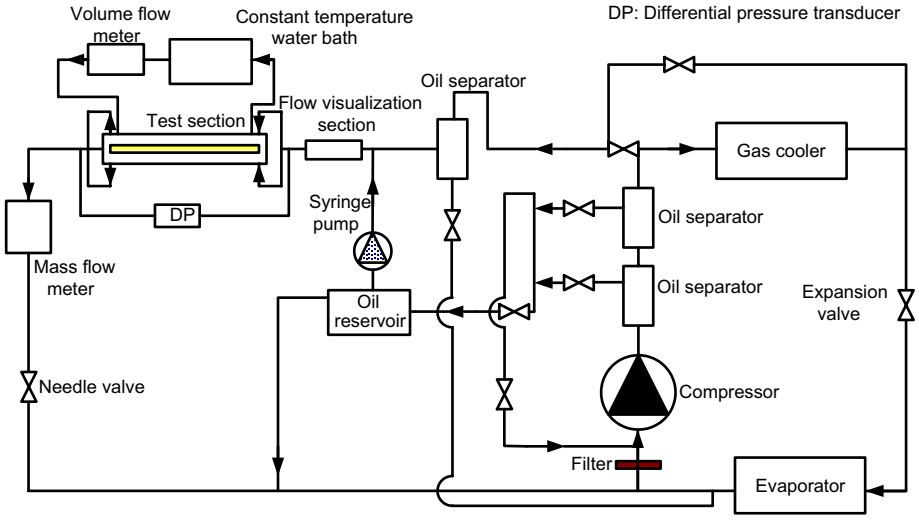

Fig. 1. Schematic of test facility.

oil to the test section. The volume flow rate was controlled by the syringe pump from 4 ml/h to 400 ml/h. Three oil separators were installed to ensure that the oil, which were separated from CO_2/oil mixture discharged from the compressor, were prevented from flowing into the test section; this way the oil was ensured to flow only into the test section from the syringe pump. The injected oil to the test section was sent back to the compressor. The flow visualization section was installed between the test section and the syringe pump to monitor the oil flow control status to the test section. Fig. 2 shows the details of the test section. The test minichannel has 10 ports whose hydraulic diameter is 1.0 mm, the width, 16 mm, and the height, 2 mm. The water channel, which was built around the microchannel, had milled grooves as shown in Fig. 2b. Fig. 2c shows the assembly of the microchannel and the water channel.

The pressures of CO_2 at the inlet and outlet of the test section were measured by pressure transducers that ranged from 0 to 20,785 kPa. It has ±0.11% accuracy of the full scale. The CO_2 and water temperatures at the inlet and outlet of the test section were measured by RTDs that have an error of 0.01 °C. The mass flow rate of CO_2 through the test section was measured by using a Coriolis mass flow meter with an uncertainty of ±0.5%. The volume flow rate of water circulating the test section was measured by a turbine flow meter that has a range of 0–40 g/s, and an uncertainty value of ±0.25% of the reading value. A differential pressure transducer with the range of 0–206.8 kPa was installed to measure the differential pressure between the inlet and the outlet of the test section. The accuracy of the differential pressure transducer is ±0.2% of the full scale. All measurements were conducted when the desired test conditions were reached in a steady state. In the tests, the mass flux was varied from 200 to 400 kg/m^2 s, the heat flux was 20 and 25 kW/m^2, and the test section inlet pressure was changed from 8.4 to 10.4 MPa. The test section

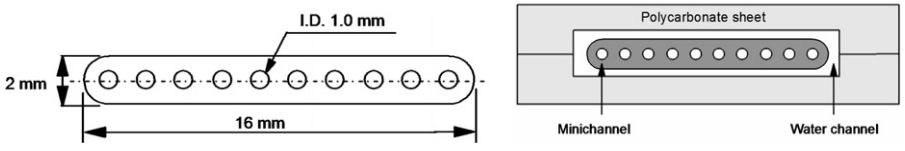

(a) Dimensions of minichannel (b) Front view of the test section

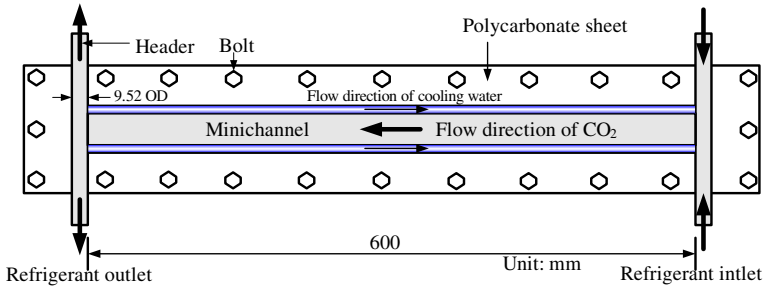

(c) Top view of the test section

Fig. 2. Details of test section.

inlet temperatures were controlled from 40 to 80 °C. The oil concentration (ω) of the test section, which was calculated from the mass flow rates by using Eq. (1), was varied in 0, 1, 2, 3, and 4 wt.%. The mass flow rate of the injected oil in Eq. (1) was calculated from the volume flow rate and oil density proposed by the oil manufacturer. Table 2 shows the oil properties of specific heat, density and dynamic viscosity at five different temperatures. The specified efficiency of each oil separator is 90% or higher. Therefore, about 0.1% of the oil or less discharged from the compressor pass over the three serially connected oil separators. This amount of oil corresponds to be less than 0.1 wt.% of oil concentration, which was estimated by considering the total flow rate of CO_2 discharged from the compressor. Moreover, the fluid flow condition was monitored through the flow visualization section after the three oil separators, confirming that the minimal amount of oil was passed over the three separators throughout the tests.

$$\omega = \frac{\dot{m}_{oil}}{\dot{m}_{mix}} \times 100 \quad (1)$$

Table 3 shows the control methods of the test conditions. The test section inlet pressures of CO_2 were controlled by adjusting the charge amount of CO_2 in the system and by adjusting the opening of the expansion valve. The temperature of CO_2 at the test section inlet was controlled by adjusting the opening of the two valves at the inlet and the outlet of the gas cooler as shown in Fig. 1. The heat transfer rate between water and CO_2 was set by regulating the test section inlet water temperature. For each test, the energy balance between water-side and CO_2-side heat transfer rates was checked and with less than 5% difference. The water-side heat transfer rate was calculated by using the following equation:

$$\dot{q}_{water} = \dot{m}_{water} c_{p,water} (T_{outlet} - T_{inlet})_{water} \quad (2)$$

Table 2
Properties of the test oil

Temperature (°C)	c_p (J/kg K)	ρ (kg/m^3)	M (N/s m^2)
0	1478	1011	0.2635
25	1567	996	0.08148
50	1656	980.6	0.03014
75	1746	965.3	0.01283
100	1835	949.9	0.006107

Table 3
Control methods of test conditions

Test conditions	Control methods of test conditions
Test section inlet pressure of CO_2	Charge amount of CO_2 in the system
	Controlling the expansion valve opening
Test section inlet temperature of CO_2	Controlling the opening of valve at gas cooler
Heat transfer rate between water and CO_2	Water temperature at test section inlet

The CO_2/oil side heat transfer rate was calculated by Eq. (3), which includes the heat transfer rate of oil.

$$\dot{q}_{co_2/oil} = \dot{m}_{co_2}(h_{inlet} - h_{outlet}) + \dot{m}_{oil} c_{p,oil}(T_{inlet} - T_{outlet}) \quad (3)$$

The uncertainty of heat transfer coefficients was calculated as summarized in Appendix A, and the average uncertainty including the precision error was 6.3%.

3. Data reduction

The CO_2-side heat transfer coefficient was calculated by Eqs. (4)–(6). Eq. (6) was obtained by using the Wilson Plot method [9]. During the Wilson Plot evaluation, CO_2 was maintained at a supercritical state with a pressure of 9.6 MPa and an inlet temperature of 54 °C. Since the accuracy of this calibration can be improved with a higher heat transfer coefficient on the CO_2 side, a higher mass flux of 980 kg/m^2 s was chosen. The calibration was conducted at 16 different water mass flow rates from 4.5 to 30 g/s:

$$\frac{1}{(hA)_{co_2}} = \frac{1}{(hA)_{overall}} - \frac{1}{(hA)_{water}} \quad (4)$$

$$(hA)_{overall} = \frac{\dot{q}}{T_{lmtd}} \quad (5)$$

$$h_{water} = 0.0466 \times Re^{0.6978} \times Pr^{0.4} \times k/d_h \quad (6)$$

4. Results and discussion

4.1. Heat transfer characteristics

Fig. 3 shows the variation of heat transfer coefficients with an average CO_2 temperature under no oil condition. Here, the average CO_2 temperature is defined as an arithmetic mean of the inlet and the outlet CO_2 temperatures

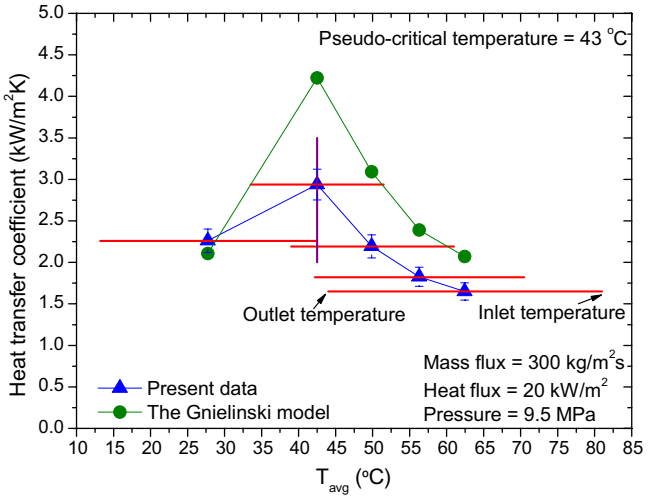

Fig. 3. Variation of heat transfer coefficient with average CO_2 temperature under no oil condition.

across the test section. The mass flux was 300 kg/m^2 s and the heat flux was 20 kW/m^2. The test section inlet pressure was kept constant at 9.5 MPa. In Fig. 3, the horizontal line at each data point shows a temperature variation of CO_2 across the test section and the vertical line shows error bars. The pseudocritical temperature is defined as the temperature at which the specific heat is the highest at the given pressure. The temperature interval of inlet and outlet CO_2 temperatures across the test section is smaller for the data points around a pseudocritical temperature than those far from it due to the higher specific heat. When the measured heat transfer coefficients were compared with the estimated values by the Gnielinski model, they show very similar trends at various average home CO_2 temperatures with an average deviation of 19%. However, a large deviation was observed around the pseudocritical temperature. It should be noted that this deviation could be different depending upon the test temperature interval of CO_2 around the pseudocritical temperature. Fig. 4 shows the effects of oil on the gas cooling heat transfer coefficients. When the oil concentration is 2 wt.%, the average heat transfer coefficients are 9.6% lower than those for 0 wt.% oil concentration. For 4 wt.% oil concentration, the degradation is 20.4% as compared to 0 wt.% oil concentration. As Dang et al. [11] reported, the oil flows in a film form at high temperature (gas cooler inlet conditions) and in a large number of droplets at low temperature (gas cooler exit conditions). When the oil flows in either droplets or oil liquid film, the oil will obstruct the heat transfer between CO_2 bulk flow and the tube wall. As the oil concentration increases, there will be more oil droplets or thicker oil film, and consequently will cause more thermal resistance. Therefore, the heat transfer coefficient decreases as the oil concentration increases. Since the specific heat (c_p) of the oil is smaller than that of pure CO_2, the c_p of the CO_2/oil mixture is lower than that of pure CO_2. Therefore, the log mean temperature difference (T_{lmtd}) in Eq. (5) of the mixture is larger than that of pure CO_2 at constant heat transfer rate, and smaller heat transfer coefficients were obtained for the mixture. Moreover, the Prandlt number and the Reynolds number of the CO_2/oil mixture were estimated to be smaller than those of the pure CO_2 when the mixture properties were averaged by the mass fraction ratio between the oil and the CO_2 such as Eqs. (9) and (10). In this study, the degradation of the heat transfer coefficients was observed to be more significant around the pseudocritical temperature than far from it. This large degradation of heat transfer coefficients around the pseudocritical temperature was also observed in Kuang et al.'s experiments [16]. This may be due to the higher effects of the oil concentration on the thermophysical properties of CO_2/oil mixture near the pseudocritical temperature. Fig. 5 shows the effects of the mass flux on the heat transfer coefficients at the same average temperature of CO_2. It is crucial to set the same average temperature of the CO_2 for each test in order to investigate the effects of the mass flux on the heat transfer coefficients because the thermophysical properties of CO_2 are critically dependent upon the temperature. Fig. 5 shows clear trends that the heat transfer coefficients increase at a higher mass flux condition under the same average temperature condition. On the other hand, the results in this study showed that the degradation ratio of the heat transfer coefficient with the oil concentration increases under the higher mass flux condition. Fig. 6 shows the effects of CO_2 pressure at the test section inlet on the heat transfer coefficients. The inlet and outlet temperatures of CO_2 at the test section were carefully controlled to the same values. When the pressure increased at the same average temperature, the heat transfer coefficient increased. This is because the average CO_2 temperature approached the pseudocritical temperature with increasing pressure.

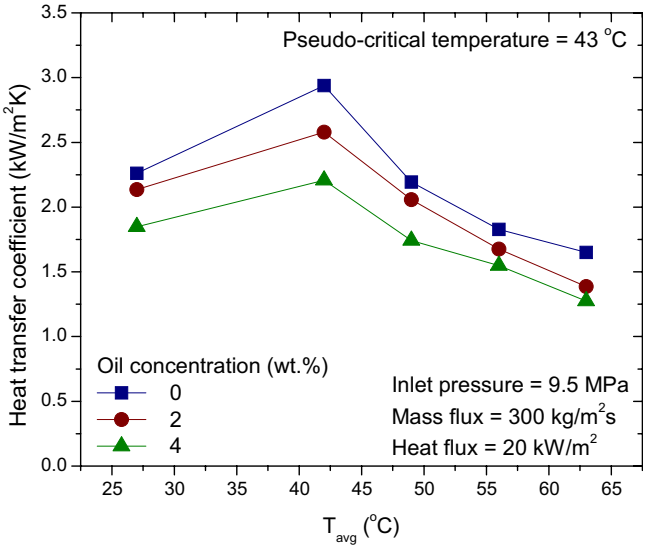

Fig. 4. Effects of oil concentration on the heat transfer coefficient.

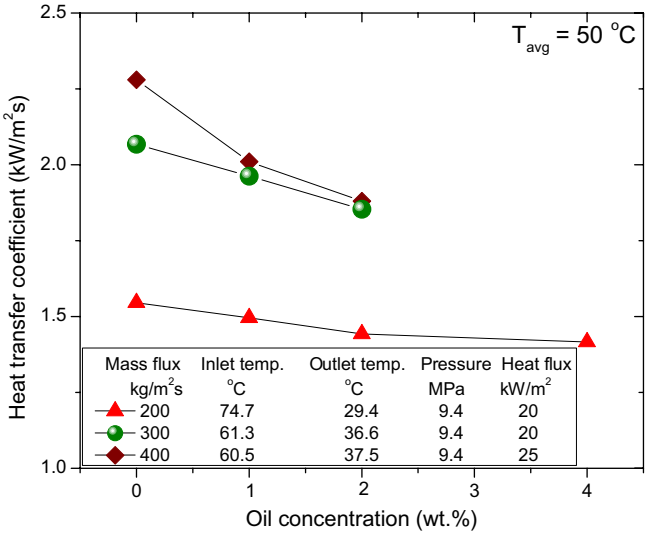

Fig. 5. Effects of mass flux on the heat transfer coefficient at various oil concentrations.

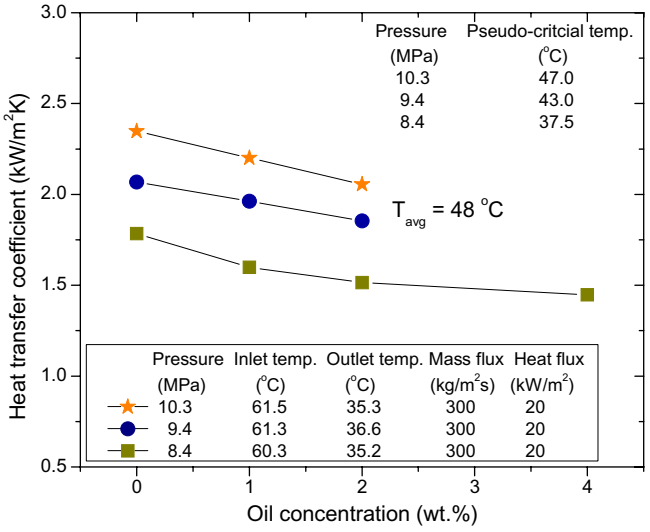

Fig. 6. Effects of inlet pressure on the heat transfer coefficient at various oil concentrations.

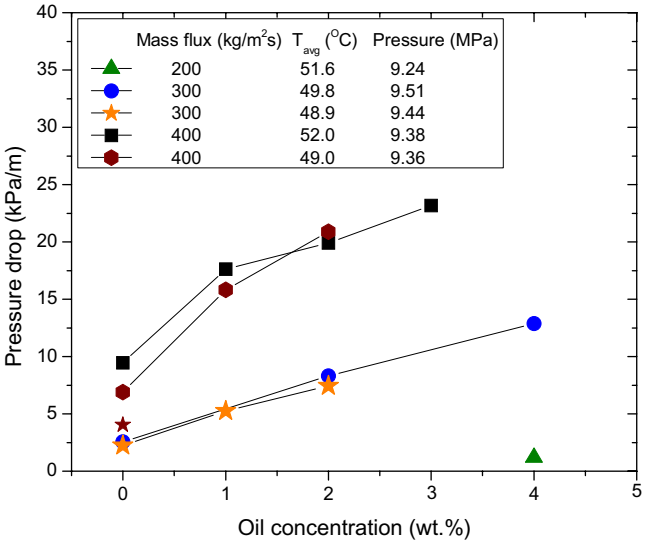

Fig. 8. Effects of mass flux on the pressure drop at various oil concentrations.

4.2. Pressure drop characteristics

Fig. 7 shows the effects of the oil concentration on the pressure drop across the test section at various average CO_2 temperatures. As shown, the pressure drop increases and the density of CO_2 decreases as the average CO_2 temperature increases. This decrease of the CO_2 density results in the increased velocity of CO_2 inside the microchannel, which consequently results in the higher pressure drop. When the effects of the oil concentration on the pressure drop are considered, the pressure drop significantly increases with the oil concentration. Fig. 8 shows the effects of the mass flux on the pressure drop at various oil concentrations. As the oil concentration increases from 0 to 2 wt.% at the same mass flux, the pressure drop increases by 2.9 times on average. When the oil concentration increases from 0 to 4 wt.%, the pressure drop increases by 4.8 times on average. This result can be explained by the flow condition as reported by Dang et al. [11]. As the oil concentration increases, there will be more oil droplets or thicker oil film. Since the viscosity of liquid oil is much higher than that of the gaseous CO_2, the oil droplets or the oil film wetting the tube wall will significantly increase the hydraulic resistance for the bulk flow. When the mass flux increases from 300 to 400 kg/m^2 s at the same oil concentration, the average pressure drop increases by 2.9 times. Fig. 9 shows the effects of the test section inlet pressure on the pressure drop at various oil concentrations. The pressure drop decreases with the increase of the test section

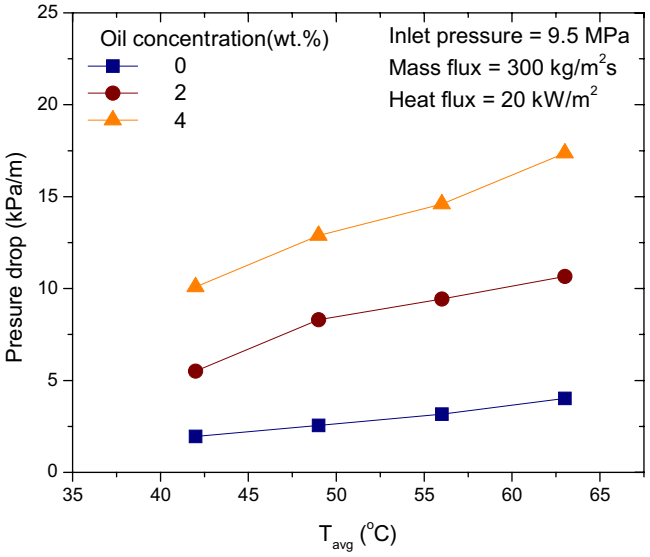

Fig. 7. Effects of oil concentration on the pressure drop at various average CO_2 temperatures.

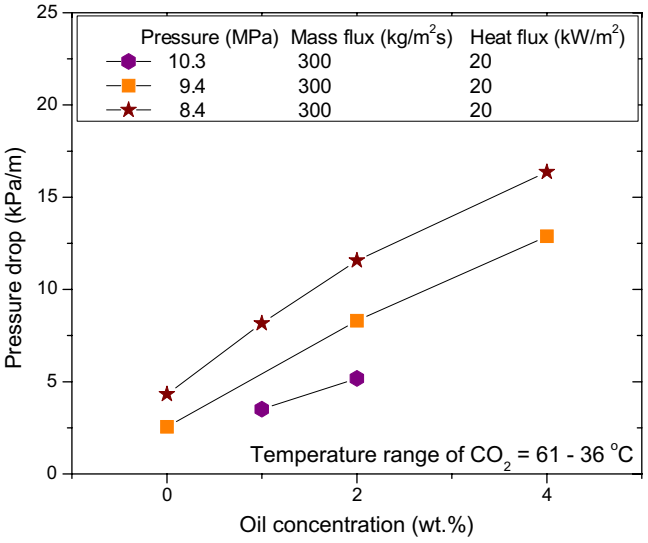

Fig. 9. Effects of inlet pressure on the pressure drop at various oil concentrations.

inlet pressure of CO_2. This trend can be also explained by the density change of CO_2 with the pressure of CO_2.

4.3. Comparison of the experimental data with the existing models

The models that predict the effects of oil on the convective gas cooling heat transfer coefficients of supercritical CO_2 are not available in the open literature. Therefore, the existing models developed for predicting the oil effects on the condensation heat transfer coefficients were used to estimate the convective gas cooling heat transfer coefficients of the supercritical CO_2 and were compared with the present data. The basic form of the existing models is shown in Eq. (7). Tichy et al. [17] used 5.0 for the constant in Eq. (7), where R12 and a 300 SUS naphthenic base oil were tested. Schlager et al. [18] suggested the constant of 3.2 in Eq. (7). The test was conducted with R22 and 150/300 SUS oil mixtures. Bassi and Bansal [19] predicted their experimental results by using the constant of 2.2 in Eq. (7). R134a and polyol ester oil were used in their experiment. Fig. 10 shows the comparison of the measured heat transfer coefficients with the predictions using the models when the oil concentration is increased from 0 to 2 wt.%. Although the predictability of each model for the degradation ratio of heat transfer coefficients with the oil concentration depends on the mass flux conditions, the Tichy et al. model [17] shows a lowest average mean deviation of 3.9% between the test results and estimated values.

$$h_{oil}/h_{no\text{-}oil} = e^{\left(-\text{const}\times\frac{\omega}{100}\right)} \tag{7}$$

There is no available pressure drop model that takes the oil effects on the pressure drops of the convective gas cooling process of supercritical CO_2 into account. The modified Darcy–Weisbach model as shown in Eq. (8) with the Blasius friction factor was used to estimate the convective

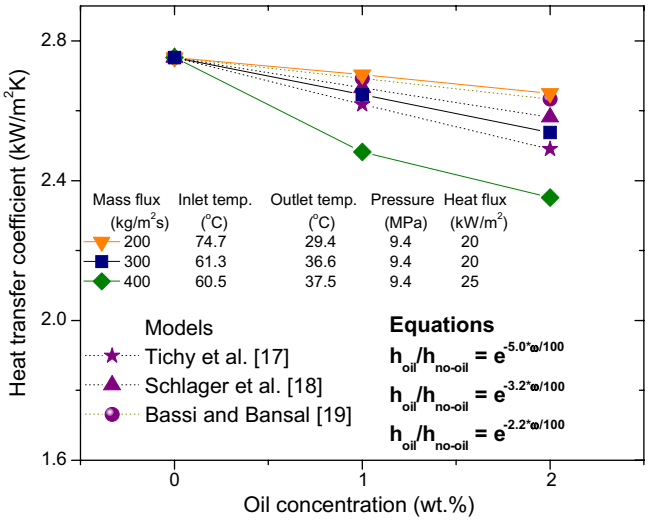

Fig. 10. Comparison of the measured heat transfer coefficients with the predictions by the existing models.

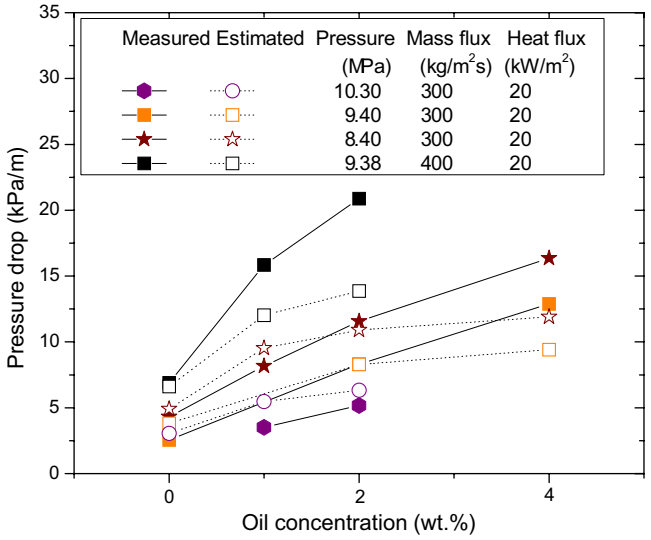

Fig. 11. Comparison of the measured pressure drops with the predictions by the modified Darcy–Weisbach model.

gas cooling pressure drops of the supercritical CO_2 and compared with the present data. K_L in Eq. (8) considered the minor losses of the pressure drops due to the contraction and expansion occurred between the headers and the microchannel, and T-junctions, which connect the headers to differential pressure transducers. The dynamic viscosity and density of the mixture in Eq. (8) are defined as Eq. (9) [20] and Eq. (10) [21], respectively.

$$\Delta P = \left(\frac{\rho_{mix}}{2}\times\left(\frac{G_{mix}}{\rho_{mix}}\right)^2\right) \times\left[\left(0.316\left(\frac{G_{mix}d_h}{\mu_{mix}}\right)^{-0.25}\times\frac{L}{d_h}\right)+K_L\right] \tag{8}$$

where

$$\mu_{mix} = \frac{\omega}{100}\mu_{oil} + \frac{(1-\omega)}{100}\mu_{co_2} \tag{9}$$

$$\rho_{mix} = \frac{\rho_{oil}}{1+\omega/100\times(\rho_{oil}/\rho_{co_2}-1)} \tag{10}$$

Fig. 11 shows the comparison between the measured data and the estimated values with the mean deviation of 23.3%. As shown in Fig. 11, the deviation between the measured and estimated values increases with the increase of the oil concentration. Eq. (8) takes into account only the change of bulk thermophysical properties of CO_2 with oil but not the effects of the oil film formed around the tube wall, which should be considered in order to better predict the pressure drop at high oil concentrations.

5. Conclusions

In this study, the effects of oil along with the test conditions, such as mass flux, test section inlet pressure and temperature of CO_2, on the convective gas cooling heat transfer

coefficients and the pressure drops in a minichannel tube operating at supercritical pressure were experimentally investigated. Significant degradation of average gas cooling heat transfer coefficients were observed up to 20.4% when the oil concentration was increased from 0 to 4 wt.%. The degradation ratio of the heat transfer coefficient increases with increase of mass flux of CO_2 at the same oil concentration. This degradation ratio was successfully estimated by using the Tichy et al. model, which was developed for predicting the effects of oil on the condensation heat transfer coefficient. As the oil concentration increases from 0 to 2 wt.% at the same mass flux, the pressure drop increases by 2.9 times in average. When the oil concentration increases from 0 to 4 wt.%, the pressure drop increases by 4.8 times in average. The modified Darcy–Weisbach model with the Blasius friction factor shows a 23.3% mean deviation between the measured data and the estimated values. The deviation increases with increase in oil concentration. Since the effects of the oil concentration on the convective gas cooling heat transfers and the pressure drops of the supercritical CO_2/oil mixture in minichannel tubes are significant, it is recommended to minimize the oil concentration to less than 0.5 wt.%.

Acknowledgements

This work was jointly supported by the sponsors of the Center for Environmental Energy Engineering (CEEE) at the University of Maryland, and the Korea Research Foundation Grant (No. M01-2005-214-10005-0).

Appendix A. Uncertainty analysis

A.1. Uncertainty of the heat transfer coefficient

The uncertainties of the gas cooling heat transfer coefficients are defined as Eq. (A.1.1). From Eqs. (4) and (5), each term in Eq. (A.1.1) can be expressed as Eqs. (A.1.2), (A.1.3), and (A.1.4).

$$W_{h_{co_2}} = \sqrt{\left(\frac{\partial h_{co_2}}{\partial h_{overall}} W_{h_{overall}}\right)^2 + \left(\frac{\partial h_{co_2}}{\partial h_{water}} W_{h_{water}}\right)^2} \tag{A.1.1}$$

$$\frac{\partial h_{co_2}}{\partial h_{overall}} = \frac{-h_{overall}}{(h_{co_2} - h_{overall}) h_{co_2}} \tag{A.1.2}$$

$$\frac{\partial h_{co_2}}{\partial h_{water}} = \frac{h_{co_2}}{(h_{co_2} - h_{overall}) h_{overall}} \tag{A.1.3}$$

$$W_{h_{water}} = W_{h_{overall}} = \sqrt{\left(\frac{\partial h}{\partial \dot{m}} W_{\dot{m}}\right)^2 + \left(\frac{\partial h}{\partial c_p} W_{c_p}\right)^2 + \left(\frac{\partial h}{\partial \Delta T} W_{\Delta T}\right)^2 + \left(\frac{\partial h}{\partial \Delta T_{lm}} W_{\Delta T_{lm}}\right)^2} \tag{A.1.4}$$

References

[1] S.S. Pitla, D.M. Robinson, E.A. Groll, S. Ramadhyani, Heat transfer from supercritical carbon dioxide in tube flow: a critical review, HVAC&R Res. 4 (3) (1998) 281–301.

[2] D.A. Olson, D. Allen, Heat transfer in turbulent supercritical carbon dioxide flowing in a heated horizontal tube, NISTIR 6234, National Institute of Standards and Technology, September 1998.

[3] S. Yoon, J. Kim, Y. Hwang, M. Kim, K. Min, Y. Kim, Heat transfer and pressure drop characteristics during the in-tube cooling process of carbon dioxide in the supercritical region, Int. J. Refrig. 26 (8) (2003) 857–864.

[4] C. Son, S. Park, An experimental study on heat transfer and pressure drop characteristics of carbon dioxide during gas cooling process in a horizontal tube, Int. J. Refrig. 29 (2006) 539–546.

[5] C. Dang, E. Hihara, In-tube cooling heat transfer of supercritical carbon dioxide. Part 1. Experimental measurement, Int. J. Refrig. 27 (2004) 748–760.

[6] S.M. Liao, T.S. Zhao, Measurements of heat transfer coefficients from supercritical carbon dioxide flowing in horizontal mini/micro channels, J. Heat Transfer 124 (2002) 413–420.

[7] S.M. Liao, T.S. Zhao, A numerical investigation of laminar convective of supercritical carbon dioxide in vertical mini/micro tubes, Prog. Comput. Fluid Dyn. 2 (2002) 144–152.

[8] C. Dang, E. Hihara, In-tube cooling heat transfer of supercritical carbon dioxide. Part 2. Comparison of numerical calculation with different turbulence models, Int. J. Refrig. 27 (2004) 748–760.

[9] J. Pettersen, R. Rieberer, S.T. Munkejord, Heat transfer and pressure drop for flow of supercritical and subcritical CO_2 in microchannel tubes, Technical Report, SINTEF Energy Research, Trondheim, February 2000.

[10] G. Kuang, M. Ohadi, Y. Zaho, Experimental study on gas cooling heat transfer for supercritical CO_2 in microchannels, in: Proceedings of the Second International Conference on Microchannels and Minichannels, Rochester, NY, 2004, pp. 325–332.

[11] C. Dang, K. Iino, E. Hihara, Flow visualization of supercritical carbon dioxide entrained with small amount of lubricating oil, in: Proceedings of the Third Asian Conference on Refrigeration and Air-conditioning, Gyeongju, May 2006, pp. 235–238.

[12] C. Dang, K. Iino, K. Fukuoka, E. Hihara, Effect of lubricating oil on cooling heat transfer of supercritical carbon dioxide, in: Proceedings of the Seventh IIR Gustav Lorentzen Conference on Natural Working Fluids, Trondheim, 2006, pp. 499–502.

[13] L. Gao, T. Honda, Experiments on heat transfer characteristics of heat exchanger for CO_2 heat pump system, in: Proceedings of the Asian Conference on Refrigeration and Air Conditioning, Kobe, 2002, pp. 75–80.

[14] K. Mori, J. Onishi, H. Shimaoka, S. Nakanishi, H. Kimoto, Cooling heat transfer characteristics of CO_2 and CO_2–oil mixture at supercritical pressure conditions, in: Proceedings of the Asian Conference on Refrigeration and Air Conditioning, Kobe, 2002, pp. 81–86.

[15] A. Zingerli, E.A. Groll, Influence of refrigeration oil on the heat transfer and pressure drop of supercritical CO_2 during in-tube cooling, in: Proceedings of the Fourth IIR-Gustav Lorentzen Conference, Purdue, IN, 2000, pp. 269–278.

[16] G. Kuang, M. Ohadi, Y. Zhao, Experimental study of miscible and immiscible oil effects on heat transfer coefficients and pressure drop in microchannel gas cooling of supercritical CO_2, in: Proceedings of 2003 ASME Summer Heat Transfer Conference, Las Vegas, NV, 2003, HT2003-47473.

[17] J.A. Tichy, N.A. Macken, W.M.B. Duval, An experimental investigation of heat transfer in forced convection condensation of oil-refrigerant mixtures, ASHRAE Trans. 91 (1985) 297–309.

[18] L.M. Schlager, M.B. Pate, A.E. Bergles, Performance predictions of refrigerant-oil mixtures in smooth and internally finned tubes, ASHRAE Trans. 96 (1990) 170–182.

[19] R. Bassi, P.K. Bansal, In-tube condensation of mixture of R134a and ester oil: empirical correlations, Int. J. Refrig. 26 (2003) 402–409.

[20] A. Cicchitti, C. Lombardi, M. Zsilvestri, G. Soldaini, R. Zavattarelli, Two-phase cooling experiments-pressure drop, heat transfer and burnout measurements, Energ. Nucl. 7 (1960) 407–425.

[21] ASHRAE, Lubricants in Refrigerant System, ASHRAE-Handbook-Refrigeration, 2006, p. 7.8.